Generation of αGFP-nanobodies suitable for super-resolution imaging of nuclear proteins

Niklas Bachmann
Wyman Group
Erasmus MC, Rotterdam
niklas@bachmann-web.de

ABSTRACT

The emergence of single molecule localization microscopy (SMLM) techniques made the imaging of cells at resolutions far beyond the diffraction barrier possible. However, the usual approach of tagging a protein of interest (PoI) with a primary antibody, and tagging this one with a fluorophore-carrying secondary antibody, introduces a significant displacement of the signal from the PoI. Here, the generation and application of an αGFP-nanobody is described which, through its reduced size and direct fluorophore labeling, leads to a much higher co-localization of signal and PoI and qualifies for dSTORM imaging of nuclear proteins.

Keywords

SMLM, dSTORM, nanobody, GFP, microscopy

INTRODUCTION

Fluorescence microscopy is a technique that exploits the quantumphysical characteristics of fluorescent molecules (FMs) and that allows imaging of proteins of interest within a cell. In short, FMs are irradiated with electromagnetic (EM) waves of certain wavelengths within the range of visible light, pushing them into an excited energy level. As the molecules return to their ground state, they emit energy again in the form of an EM wave of a slightly longer wavelength, which can then be detected. However, as described by Abbe's Law, the minimum distance between two points with overlapping signals needed to still be distinguishable is directly proportional to their wavelength, which leads us to a resolution limit for conventional fluorescence microscopy of about a third of the wavelength of the laser[1].

Single molecule localization microscopy (SMLM) techniques break this so-called diffraction barrier. In the case of direct stochastic optical reconstruction microscopy (dSTORM) this is done by taking advantage of another, more stable energy level called the dark state, that leads to a large portion of FMs to be 'switched off' and only stochastically return to a fluorescent state, resulting in the individual detection of single molecules with a precision of tens of nanometers[2]. This technique relies heavily on particular characteristics of fluorophores such as their ratio between OFF and ON time and the number of switching cycles they can go through before permanent photobleaching. Furthermore, while extremely high resolution can be achieved, FMs are usually conjugated to secondary antibodies, which introduces significant label displacement and thus the detected signal can still be around 30nm from the actual location of the protein of interest, making it hard to determine the exact morphology and structure of complexes such as protein filaments on DNA[3]. Nanobodies are antibody fragments consisting of only the epitope-binding domain, which are considerably smaller with a diameter of around 2-4nm[4]. Here, the generation of a GFP-specific nanobody labeled with far-red fluorescent dye suitable for STORM imaging is described, which can be used to produce super-resolution images of even nuclear proteins that are tagged with GFP with minimal label displacement.

MATERIALS AND METHODS

αGFP-nanobody expression and purification

The pOPINE GFP nanobody was a gift from Brett Collins (Addgene plasmid # 49172)[5]. An additional Cysteine residue was introduced at the C-terminus through PCR, as well as a His6-tag and a TEV cleaving site at the N-terminus, and the PCR fragment was then cloned into a pETM-11 carrier plasmid with a kanamycin-resistance selection marker through Gibson assembly[6]. The nanobody contains two internal (at positions 23 and 79) and one additional Cysteine residue that was inserted at the C-terminus. The maleimide-conjugated far-red fluorescent dye used in this project can react with the accessible additional thiol group of the inserted Cys-residue in order to label the nanobody. A carrier plasmid (pETM-11) was digested with NcoI and XhoI restriction enzymes and column purified with Zeba SpinColumns. For the assembly reaction, 1µL of linearized plasmid DNA and 1µL of the nanobody insert were added to 2µL of 2x Gibson Assembly mix and then heated to 50°C for 1h. The plasmid was then amplified in E. coli (strain DH5a). The 4µL reaction volume were mixed with 50µL of cells, put on ice for 30 minutes, then heat shocked at 42°C for 45 seconds. Subsequently, 800µL of LB was added and the cells were incubated for 1h at 37°C. The transformed bacteria were grown overnight on LB-Kanamycin plates. 10 single colonies were resuspended in 2.5mL LB-Kanamycin and again incubated overnight at 37°C. Plasmid DNA was subsequently extracted through miniprep. Successful insertion of the nanobody sequence at the target site was confirmed by a restriction digest reaction and Sanger sequencing.
The retrieved plasmid was used to transform E. coli (strain BL21) in a similar fashion for a 5mL overnight culture in selective medium. The culture was then diluted into 1L

selective medium and incubated at 37°C until it reached log-phase. 0.5mM IPTG (final concentration) was added to induce protein expression for 19h at 20°C. The culture was centrifuged and the pellet was resuspended in equal volume of lysis buffer (500mM NaCl, 20mM HEPES, 10mM Imidazole, 0.5mM DTT, 1x c0mplete protease inhibitor). After 45 min of ultra-centrifugation at 60,000x g, 1.5mL Ni-NTA Agarose beads (Invitrogen) were added to the supernatant and mixed for 1h at 4°C. The sample was added to a separating column, washed twice with washing buffers (20mM HEPES, 0.5M DTT, and 500mM NaCl with 20mM Imidazole or 250mM NaCl with 40mM Imidazole respectively) and finally eluted in 17 fractions of 1mL each with an elution buffer (250mM NaCl, 20mM HEPES, 250mM Imidazole, 0.5mM DTT). The fractions with the highest amount of nanobody were pooled and stored at -80°C.

Conjugation of nanobody and fluorescent dye

For the labeling reaction, 340µL of protein (40nmoles) were first reduced by adding 60µL of 100mM TCEP, resulting in a final concentration of 15mM, for 10 min on ice. Next, the buffer was exchanged into maleimide labeling buffer (0.1M potassium phosphate, 150mM NaCl, 1mM EDTA, 2.5mM sucrose, pH 6.4[3]) using ZebaSpin Columns (MWCO 7kDa, ThermoFisher). 12µL of CF647 maleimide dye (10mM in anhydrous DMSO, Biotium) was added, leading to a 3x molar excess in dye. Immediately upon thorough mixing, 60µL 1M K_2HPO_4 were added to neutralize the reaction by raising the pH to 7.5. The sample was left on ice for 1.5h before applying it to a VivaSpin concentrator column (MWCO 5kDa, SigmaAldrich) for buffer exchange into phosphate-buffered saline (PBS), clearance of free dye and concentration of the sample.

Verification of GFP-binding activity

To confirm that the fluorescent label does not impair the binding capacity of the nanobody to GFP, size-exclusion chromatography was performed using an ÄKTAmicro FPLC system with an S75 column with an approximate volume of 2.4mL. Here, larger molecules elute sooner from the column and can be detected by measuring the absorbance at particular wavelengths. After washing with PBS, 5 samples were injected and analyzed separately based on the absorbance at 280nm (protein), 488 nm (GFP) and 650nm (fluorescent dye). The samples inserted contained 2µM GFP, 2.5µM αGFP-nanobody, 2.5µM labeled nanobody, or mixtures of GFP with labeled or GFP with unlabeled nanobody respectively at the same concentrations in 60µL PBS. GFP-binding activity of the labeled nanobody would be visualized as a shift of the 488nm absorbance peak (GFP) and a shift of the original peak for absorbance at 650nm (fluorescent dye) towards a second peak that overlaps with the 488nm peak, as the larger GFP-nanobody complex would elute from the column sooner.

Immunostaining

The αGFP-nanobody was tested in mouse embryonic stem (mES) cell lines (strain IB10) expressing PCNA-GFP or BRCA2-GFP, both nuclear proteins, but expressed at different protein levels (BRCA2 estimated at around 3-15nM in mES cells[7]). For control purposes, cells were alternatively stained with commercial αGFP-nanobody-ATTO647 (GFP-Booster ATTO647N, Chromotek, 1:300), which is not suitable for dSTORM imaging. All cells were fixed for 15 minutes with 2% paraformaldehyde prior to staining. However, De Groever et al. (2010) show that due to its small size, the nanobody can also be applied in in vivo imaging[8].

$0.5x10^6$ cells were seeded overnight on 24mm glass cover slips (thickness 170µm) coated with laminin. They were fixed for 15 minutes with 2% paraformaldehyde in PBS. They were permeabilized by washing them three times short and twice for 10 minutes with 0.1% PBS+triton-X100 (SigmaAldrich), and subsequently incubated for blocking at room temperature with PBS + 2% BSA + 0.15% glycerol for 30 minutes in order to minimize non-specific binding of the nanobody. The cover slips were incubated face-down on 150µL droplets of the blocking solution containing 50nM of the labeled nanobodies in a dark box for 30 minutes. Finally, the cells were washed again with PBS+triton-X100 and the cover slips were stored at 4°C in PBS.

Confocal and dSTORM imaging

Confocal and super-resolution imaging was performed using a Zeiss Elyra PS.1 microscope with an alpha Plan-Apochromat 100x oil immersion objective (numerical aperture 1.46) and the ZEN 2012 SP5 FP1 software. The signal was detected with an EMCCD Andor iXon DU 897 camera with an effective pixel size of 100*100nm.

For confocal imaging, the cover slip was loaded onto a microscope ring and 1mL of PBS was added. Images were taken with a bandpass filter (650-700nm) as z-stacks of 11 slides with a distance of 0.45µM, and for visualization of the foci, the maximum projection of this image stack was generated in ImageJ[9].

In the case of dSTORM imaging, a 655nm long-pass filter was used for the detection of the αGFP-nanobody-CF647. In order to increase the stability of the dark state for dSTORM imaging, the cells were loaded onto the microscope ring in 2 mL dSTORM buffer (containing 10% glucose, 50mM TRIS, 5mM NaCl, 25mM MEA and an oxygen scavenging compound consisting of glucose oxidase and catalase) and covered with an additional glass cover slip to reduce the contact with air and possible uptake of new oxygen. A 642nm laser was used to excite the CF647 dye and the intensity was adjusted until blinking of the molecules could be observed. A 405nm laser was added when necessary, as it has been shown that electromagnetic waves around 400nm are suitable for reverting molecules from the dark state to the fluorescent state[2]. dSTORM images were taken in time series of 20,000 frames with an exposure time of 25ms and with the illumination source at a TIRF angle between 63° and 65°.

RESULTS

Nanobody labeling and functionality

In order to determine the efficiency of the labeling reaction, SDS-polyacrylamide gel electrophoresis was performed. The labeled and unlabeled nanobody were visible in separate bands due to a difference in size and could be visualized by staining with colloidal coomassie. The intensity of the bands was measured in ImageJ three times, corrected for background, averaged, and the labeling efficiency could be calculated as the ratio of intensity of labeled to unlabeled nanobody. By this method, labeling efficiencies between 60-70% were determined.

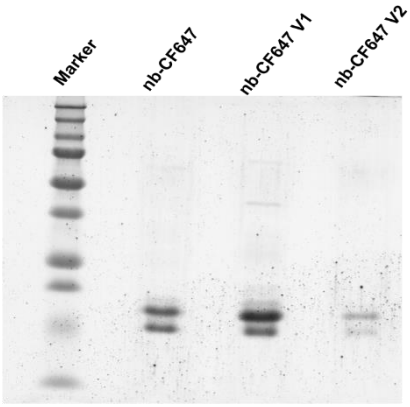

Figure 1: SDS-PAGE stained with colloidal coomassie. V1 and V2 describe the first and second round of the VivaSpin column. The upper band shows the labeled and the lower band unlabeled nanobody.

The GFP-binding activity of the labeled nanobody was tested as described above (Fig. 2). As expected, mixing GFP with the αGFP-nanobody resulted in a shift of the 488nm peak as well as a partial redistribution of the 650nm peak, co-localizing with the 488nm peak, which indicates that binding takes place. The second peak in the 650nm adsorption graph represents unbound αGFP-nanobody-CF647, caused by a molar excess and a binding efficiency below 100%, and could possibly shrink by adjusting the molar ratios and a longer incubation time before injection into the column. The observed binding activity was similar to that of unlabeled nanobody (data not shown).

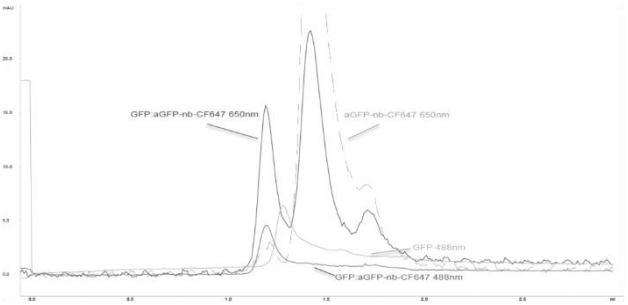

Figure 2: Adsorption peaks of size-exclusion chromatography of 2µM GFP and 2:2.5µM GFP: αGFP-nanobody-CF647 mixture. The y-axis describes the absorbance in mAU, the x-axis shows the eluted volume in mL.

Qualification of the labeled nanobody for dSTORM imaging

PCNA-GFP or BRCA2-GFP expressing cells were immunostained and prepared as described above.

For both PCNA and BRCA2, foci were clearly visible under the confocal microscope (Fig. 3). The absence of foci in the wild-type cells indicates that the αGFP-nanobody does not show any non-specific binding activity.

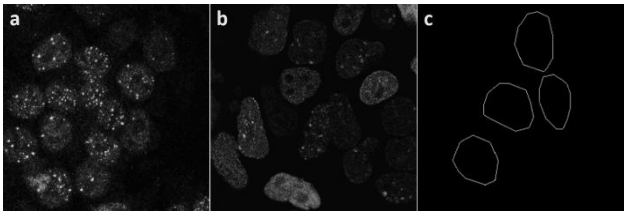

Figure 3: Maximum projections of z-stack from confocal imaging: staining with 50nM αGFP-nanobody-CF647 of mouse ES cells expressing BRCA2-GFP (a), PCNA-GFP (b) or no GFP-tagged protein (wild-type, c)

The detected CF647-signal co-localized with the GFP. The signal quality and patterning of the foci were similar to a control using a commercial αGFP-nanobody-ATTO647 construct, which is not as suitable for dSTORM imaging, but the cells stained with the nanobody-CF647 showed a stronger background fluorescence (Fig. 4).

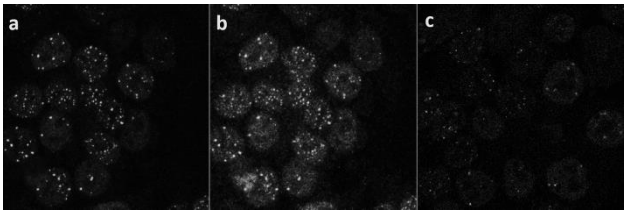

Figure 4: Maximum projections of z-stack from confocal imaging of BRCA2-GFP expressing mouse ES cells: GFP signal (a), αGFP-nanobody-CF647 (b), αGFP-nanobody-ATTO647 (c). *a* and *b* show the same field of view.

BRCA2-GFP expressing and wild-type cells were also stained with 50nM of free CF647 dye and with PBS as a negative control to exclude autofluorescence as a cause of background fluorescence (Fig. 5). The absence of any signal in the control but evenly distributed fluorescence in the nucleus in the cells stained with CF647 leads to the assumption that the background signal observed in the cells stained with the labeled nanobody is caused by free dye that has not fully been eliminated in the sample.

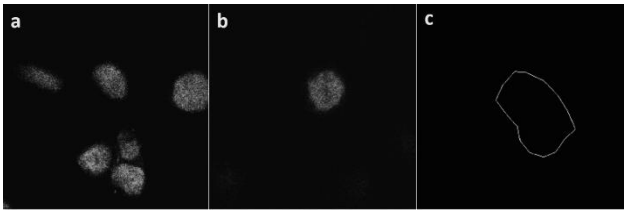

Figure 5: Maximum projections of z-stack from confocal imaging: BRCA2-GFP expressing mouse ES cells (a) and WT mouse ES cells (b) stained with 50nM CF647 dye, negative control of WT mouse ES cells with PBS (c).

dSTORM imaging of BRCA2-GFP cells with αGFP-nanobody-CF647 gave sufficient signal with mean and median precision levels of around 25nm, similar to those observed when imaging RAD51 using commercial

αRabbit F(ab')2-CF568 antibody (SigmaAldrich), and could successfully be used for the detection and analysis of the morphology of BRCA2 structures at DNA damage sites in mES cells (Fig. 6).

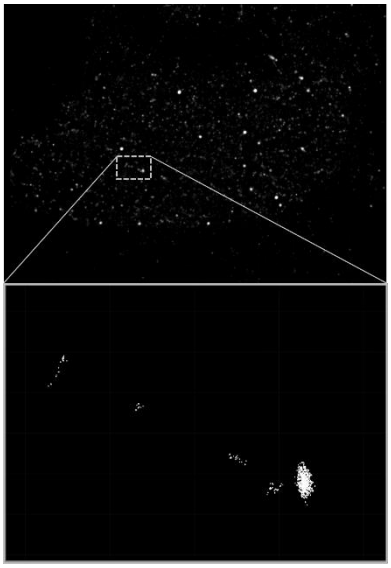

Figure 6: (a) dSTORM image of mES cell expressing BRCA2-GFP and stained with αGFP-nanobody-CF647 2h after treatment with 5Gy ionizing radiation, corrected for drift and with a signal intensity threshold of 2x standard deviation. (b) Discrete localizations of CF647 signal in the indicated section after filtering by means of a precision threshold and Voronoi tessellation.

CONCLUSION

The αGFP-nanobody-CF647 construct provides an easy way to image any GFP-tagged protein in a cell. The expression in and purification from E. coli cultures makes it a fast and cost-efficient procedure that doesn't require any additional animal sacrifice and is easily reproducible. The labeling reaction follows a simple protocol and since the fluorescent dye is directly conjugated with the nanobody, there is no need for a secondary antibody, which makes the immunostaining protocol faster and cheaper. The final construct still showed GFP-binding activity comparable to the unlabeled nanobody, indicating that the dye does not affect the interaction with the target protein. With GFP being a widely used fluorescent protein, many cell lines for GFP-tagged proteins of interest already exist or can be generated comparably easily, which allows for the use of this contruct in a wide variety of target proteins. Due to its suitability for dSTORM imaging, the described nanobody construct can be used to generate super-resolution data with extremely high precision while minimizing the significant loss in accuracy caused by the label displacement that comes with the use of antibodies.

In order to further improve the labeling efficiency, different adjustments to the labeling buffer or further purification, reduction and similar preparation steps could be tested. The free dye causing background signal could be better eliminated by more or different purification columns, or by gel-filtration, where the free dye would elute from the resin separately from the labeled nanobody due to the large size difference. Furthermore, a more suitable blocking solution, with blocking agents that have chemical structures more similar to that of the dye, might further reduce the background signal caused by sticky free dye. In this project, the nanobodies were not tested for the ability to penetrate the nuclear membrane *in vivo*, which would be useful for life cell imaging of nuclear processes.

ROLE OF THE STUDENT

Niklas Bachmann was an undergraduate student working under the supervision of Maarten Paul when the research in this report was performed. The assembly of the nanobody-expression plasmid and amplification as well as expression and purification were performed by the student. Protocols for fluorescent dye conjugation and immunostaining existed but were optimized by the student. All cell lines used in this experiment were generated prior to the beginning of this project by other members of the Wyman Group. The design of the experiments for verification of the functionality of the nanobody was done partly by Maarten Paul, partly by the student, and all experiments were conducted by the student after initial instructions by Maarten Paul.

ACKNOWLEDGMENTS

I thank Claire Wyman for the opportunity of learning and working in her lab, Maarten Paul for the guidance and support over the entire course of the project, and Tate Marshall for all the mental support in- and outside the lab.

REFERENCES

[1] Abbe, E. Beiträge zur Theorie des Mikroskops und der mikroskopischen Wahrnehmung. *Archiv für Mikroskopische Anatomie 9* (1873), 413–418

[2] Single-Molecule Super-Resolution Imaging https://www.microscopyu.com/techniques/super-resolution/single-molecule-super-resolution-imaging

[3] Pleiner, T. et al. Nanobodies: site-specific labeling for super-resolution imaging, rapid epitope-mapping and native protein complex isolation. *eLife 2015;4:e11349*

[4] Van Audenhove, I. and Gettemans, J. Nanobodies as Versatile Tools to Understand, Diagnose, Visualize and Treat Cancer, *EBioMedicine 8* (2016), 40-48.

[5] Kubala, M. H., Kovtun, O., Alexandrov, K. & Collins, B. M. Structural and thermodynamic analysis of the GFP:GFP-nanobody complex. *Protein Science 19* (2010). doi:10.1002/ pro.5199

[6] Gibson, D. G. et al. Enzymatic assembly of DNA molecules up to several hundred kilobases. *Nature Methods 6* (2009), 343-345.

[7] Reuter, M. et al. BRCA2 diffuses as oligomeric clusters with RAD51 and changes mobility after DNA damage in live cells. *Journal of Cell biology* 207. (2014).

[8] De Groeve, K. et al. Nanobodies as Tools for In Vivo Imaging of Specific Immune Cell Types. *Journal of Nuclear Medicine, 53* (2010), 782-789.

[9] Schindelin, J. et al. Fiji: an open-source platform for biological-image analysis. *Nature Methods 9* (2011), 676-682.